SIMULATION STUDY ON HYBRID ELECTRIC PROPULSION SYSTEM OF EXTENDED RANGE AMPHIBIOUS VEHICLE USING MATLAB/SIMULINK

Nguyen Van Tong Em[1,2], Nguyen Van Trang[1]*, Le Tat Hien[3,4]

[1]*Ho Chi Minh City University of Technology and Education, Vietnam*

[2]*Nam Can Tho University, Vietnam*

[3]*Ho Chi Minh City University of Technology, Vietnam*

[4]*Vietnam National University Ho Chi Minh City, Vietnam*

*Corresponding author: trangnv@hcmute.edu.vn

(Received: March 27, 2025; Revised: May 05, 2025; Accepted: May 23, 2025)

DOI: 10.31130/ud-jst.2025.23(6A).165E

Abstract - This study proposes the design of an extended-range amphibious vehicle equipped with a self-sustaining power system to support the electric propulsion system and enhance the operational range of the vehicle. The system includes a 10 kW generator driven by an internal combustion engine. A simulation model was developed in MATLAB/Simulink to evaluate the vehicle's performance. Simulation results under land-based operating conditions indicate that the vehicle achieves a maximum speed of 60 km/h and accelerates from 0 to 40 km/h in 15.6 seconds with a 7.5 kW motor. The model also analyzes engine power, battery power, generator power, battery state of charge, and charging current at various speed levels. The self-sustaining energy system enables the vehicle to echarge its 72 V, 120 Ah battery at a maximum rate of 0.2C during deceleration or when stationary. The findings demonstrate the feasibility of the proposed model and its potential for practical application.

Key words - Extended-range amphibious vehicle; Self-sustaining energy system; MATLAB/Simulink

1. Introduction

With the depletion of non-renewable oil resources, the traditional automotive industry faces significant challenges due to fuel shortages, contributing to a global energy crisis [1]. The automotive sector remains a vital component of the global economy and has undergone substantial growth, driven by technological advancements. Beyond conventional land and water-based transportation, amphibious vehicles capable of operating in both environments have been the subject of increasing research and development in recent years. These vehicles serve a wide range of applications, including military operations, search and rescue missions, tourism, and recreation, offering enhanced mobility across diverse terrains [2-3]. However, conventional vehicles, particularly those powered by internal combustion engines, remain a major source of environmental pollution. The combustion of fossil fuels releases various pollutants, including carbon monoxide (CO), hydrocarbons (HC), nitrogen oxides (NOx), and particulate matter (PM), which have caused significant environmental degradation and ecosystem disruption [4-5]. To mitigate pollution and reduce reliance on fossil fuels, the transportation sector is increasingly prioritizing the development of clean energy vehicles, particularly pure electric vehicles (PEVs). These vehicles not only minimize emissions but also demonstrate higher energy efficiency compared to conventional internal combustion engine vehicles [6-7]. However, a major limitation of PEVs is their restricted driving range, primarily due to the current constraints of battery technology, which has yet to achieve sufficient energy density for extended operation. In contrast, hybrid electric vehicles (HEVs) offer improved fuel efficiency and lower emissions, making them a viable transitional solution between conventional and fully electric vehicles [8]. Consequently, advancements in renewable energy integration and energy storage technologies will play a crucial role in shaping the future of sustainable transportation [9].

To address the limitations of pure electric vehicles, Extended Range Electric Vehicles (EREVs) have emerged as promising solutions to overcome driving range constraints. These vehicles incorporate a range-extending system that utilizes a small internal combustion engine and a generator to supply power to the electric motor when the battery is depleted, thereby enhancing the vehicle's range without concerns about distance limitations [10-11]. This study investigates the application of a hybrid powertrain system with an extended range for amphibious vehicles, specifically designed to support eco-tourism development in Vietnam. The proposed vehicle adopts a powertrain architecture similar to that of pure electric vehicles but integrates a range extender comprising a small internal combustion engine and a generator to supply additional power when required [12]. The design model will be developed and simulated using MATLAB/Simulink to optimize the performance of the amphibious vehicle and facilitate real-world implementation, particularly in eco-tourism areas of the Mekong Delta region.

To conduct this research, key parameters, including electric motor power and battery discharge rate, will be determined based on fundamental automotive principles. The electric motor power will be calculated by considering factors such as vehicle weight, road gradient, and acceleration requirements, while the battery discharge rate will be assessed to ensure sufficient energy supply for a specified driving range. Once these parameters are defined, a simulation model of the electric amphibious vehicle with a range extender will be developed in the MATLAB/Simulink environment. This model will simulate the vehicle's operation on land, incorporating both the electric motor and the range-extending system. Performance metrics such as vehicle acceleration, energy consumption, range extender efficiency (including the power output of the internal combustion engine and generator), operating current, and battery charging current during range extender operation will be evaluated.

2. Design and modeling of an extended-range amphibious vehicle

2.1. Design an Extended-Range Amphibious Vehicle

Figure 1 illustrates the schematic configuration of the hybrid powertrain system developed for the extended-range amphibious vehicle. The system is centered around an electric motor, which functions as the primary propulsion source during both terrestrial and aquatic operation modes. The energy required by the motor is supplied by a high-voltage battery pack that stores electrical energy and ensures reliable power delivery. This battery can be recharged through two main sources: externally from the power grid or internally via an onboard range extender. The range extender consists of a gasoline-powered internal combustion engine (ICE) mechanically coupled to an electric generator and inverter, forming an auxiliary generation unit.

Additional key components of the system include an electric coupling device, an engine control unit (ECU), and a torque distribution mechanism, which enables seamless switching and efficient torque allocation between land and water propulsion modes. Notably, there is no mechanical linkage between the ICE and the driveline; as such, the ICE's sole purpose is to generate electrical energy. This architecture allows the ICE to operate within its optimal efficiency range, independent of vehicle speed or load conditions. The activation and deactivation of the range extender are governed by several dynamic factors, including the battery's state of charge (SOC), instantaneous power demand from the driver, vehicle velocity, and a predefined energy management strategy.

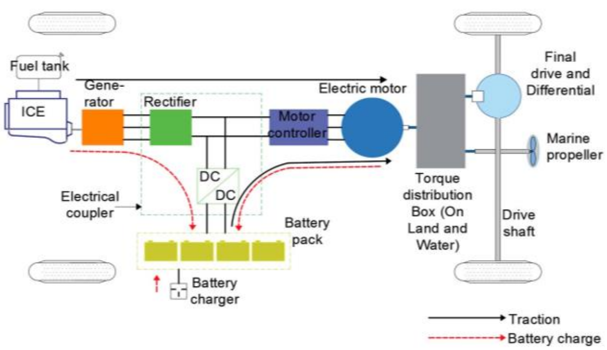

Figure 1. *The diagram of the hybrid powertrain system for the extended-range amphibious vehicle*

2.2. Calculation and selection of parameters for the hybrid powertrain system of the extended-range amphibious vehicle

The parameter design for the hybrid powertrain system of the amphibious vehicle aims to ensure that the vehicle meets the desired performance criteria, including maximum speed, acceleration capability, hill-climbing performance, and other technical specifications. Key components of the powertrain system, including the electric motor, range extender (comprising a compact internal combustion engine and generator), high-voltage battery, and electric couplings, are meticulously calculated and engineered. These components serve as the core elements of the hybrid powertrain system, ensuring stable and efficient operation while meeting performance requirements.

2.2.1. Calculation and Selection of Electric Motor and Generator

Table 1. *The parameters, design specifications, and basic technical specifications of the amphibious vehicle*

Parameters	Values
The number of passengers, including the driver	4
Air density (ρ_a)	1.25 kg/m^3
Drag coefficient (C_D)	0.5
The frontal area of the vehicle (A_f)	1.65 m^2
Gravitational acceleration (g)	9.81 m/s^2
Rolling resistance coefficient (f_r)	0.013
Total vehicle mass (m)	860 kg
Wheel radius (r_w)	0.3 m
Maximum speed on land	60 km/h
Average speed on land	40 km/h
Maximum slope angle	≥ 20
Gearbox ratio	6.12

The parameters, design specifications, and basic technical specifications of the amphibious vehicle are shown in Table 1. Similar to pure electric vehicles, the rated power of the electric motor in the hybrid powertrain system of the extended-range amphibious vehicle is determined based on the acceleration performance requirements of the amphibious vehicle, as well as the characteristics of the electric motor and the driveline. The maximum speed of the amphibious vehicle is V_{max}=60 km/h, and the time required to accelerate the vehicle from 0 to 40 km/h should not exceed 25 seconds. The power of the electric motor is determined by equation (1) [13]:

$$P_t = \frac{\delta.M}{2t_a}\left(V_f^2 + V_b^2\right) + \frac{2}{3}M.g.f_r.V_f + \frac{1}{5}\rho_a.C_D.A_f.V_f^3 \quad (1)$$

where t_a is the expected acceleration time (s), V_b is the vehicle speed (m/s), and V_f is the vehicle's base speed during acceleration (m/s). Based on practical considerations, the engine parameters for the electric motor are selected as shown in Table 2.

Table 2. *Technical specifications of the electric motor*

Parameters	Values
Model	GEV1042MA
Rated power	7.5 kW
Maximum speed	6500 rpm
Rated torque	47 Nm
Rated current	250 A
Rated efficiency	90%
Maximum torque	108 Nm
Maximum power	19 kW

In this study, the internal combustion engine and generator will operate under different conditions, providing power to support the amphibious vehicle during the range extension phase. Therefore, the internal combustion engine will operate in optimal mode to meet the speed requirement of the amphibious vehicle at 60 km/h, as determined by the following equation [13]:

$$P_{e/g} = \frac{V}{1000\eta_t.\eta_m}\left(M.g.f_r + \frac{1}{2}.\rho_a.C_D.A_f.V^2\right)(kW) \quad (2)$$

where: η_t, η_m, and η_g represent the efficiencies of the transmission system, electric motor, and generator, respectively.

The power for the range extender (internal combustion engine/generator) is selected to provide energy to the high-voltage battery in a stable state to prevent the battery from being fully discharged, while also maintaining the optimal state of charge (SOC) of the high-voltage battery. It must be compatible with the power requirements of the electric motor it supports. In practice, the output power of the internal combustion engine/generator is typically selected chosen to be 10-25% higher than the actual power demand of the electric motor to enhance the lifespan and durability of the generator. Based on practical considerations, we will select the Shineray SG12000E gasoline-powered generator with the specifications listed in Table 3.

Table 3. *Technical Specifications of the Shineray SG12000E Gasoline Engine/Generator*

Parameters	Values
Maximum power of an Internal Combustion Engine	15 kW (3600 rpm)
Maximum generator power	10.5 kW
Dimensions (length x width x height)	98.5 x 65.6 x 75 cm
Weight	189 kg

2.2.2. Design of Battery Parameters

To maximize the electric motor's power output, the total power of the range extender system (internal combustion engine/generator) and the battery must be greater than or at least equal to the rated maximum power of the electric motor. The capacity of the high-voltage battery is determined as follows [13]:

$$P_{PPS} \geq \frac{P_{m,max}}{\eta_m} - P_{e/g} \quad (3)$$

where $P_{m,max}$ is the rated maximum power of the motor, ηm is the efficiency of the motor, and Pe/g is the power of the internal combustion engine/generator at its designed operating point.

Based on practical considerations, , the selected power for the primary power source (P_{pps}) is 9 kW. According to the equation P_{pps} = U.I, the corresponding current is calculated as $I = \frac{P_{pps}}{U} = \frac{9000}{72} = 125$ A. Six battery packs, each with a capacity of 120 Ah and a nominal voltage of 12 V, are connected in series to achieve a total output voltage of 72 V.

2.3. Calculation and selection of parameters for the hybrid powertrain system of the extended-range amphibious vehicle

Based on the extended-range amphibious vehicle design, the MATLAB Simulink model comprises several critical components that work together to simulate the vehicle's operation accurately. The model starts with a battery rated at 72 V and 120 Ah, which is essential for providing the necessary electrical energy. This battery is connected to a DC-DC converter, which ensures a stable power supply to the DC motor. To transmit power to the driving wheels, the DC motor is linked to a gearbox. This gearbox is designed to increase the torque transmitted to the driving wheels, ensuring efficient power delivery and improved vehicle performance.

The Vehicle Body Subsystem in the Simulink model plays a critical role in simulating the physical characteristics and resistive forces acting on the vehicle during operation. It accounts for key factors such as vehicle weight, rolling resistance, slope resistance, and aerodynamic drag, all of which significantly influence vehicle performance and energy consumption. Environmental conditions, including road gradient and wind speed, are incorporated through the Slope and Wind Input Subsystem. This subsystem enables the model to dynamically adapt to varying external conditions, allowing for a comprehensive analysis of the vehicle's behavior across different operating scenarios.

A key component of the extended-range vehicle is its energy management system, which includes a battery charging mechanism. This system integrates an internal combustion engine (ICE) that drives a generator, producing electrical power that is regulated through a DC-DC converter to charge the battery. This configuration ensures a sustained battery charge, thereby extending the vehicle’s operational range beyond the limitations of battery capacity alone.

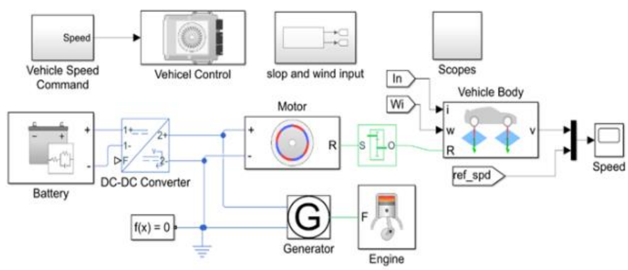

Figure 2. *The extended-range vehicle’s MATLAB/Simulink mode*

The vehicle’s speed over time is regulated by the Vehicle Speed Command Subsystem, which allows users to define a desired speed profile for the simulation. This speed command is transmitted to the Vehicle Control Subsystem, which manages the torque output of the drive motor to achieve the specified speed. The Vehicle Control Unit (VCU) utilizes real-time feedback from the vehicle’s actual speed and other operational parameters to dynamically adjust motor torque. This closed-loop control mechanism ensures that the vehicle maintains the target speed while adapting to variations in load, road conditions, and external factors. Figure 2 presents the simulation model of the extended-range amphibious vehicle developed in this study.

In this simulation, the control strategy involves transmitting the desired speed signal from the Vehicle Speed Command Subsystem to the VCU. The VCU processes this signal and converts it into angular velocity and torque commands, which are used to regulate the electric motor via a Proportional-Integral (PI) controller. The ICE, which powers the generator, is activated when the SOC of the battery drops below 50% and deactivated when the SOC exceeds 80%. To maximize fuel efficiency, the ICE operates at a constant speed of 3000 RPM. This control strategy enhances energy management by maintaining the battery within an optimal SOC range, thereby improving both vehicle performance and driving range. Figure 3 presents the VCU subsystem developed in this study, which implements a hybrid powertrain energy management algorithm. This algorithm synchronizes SOC regulation with propulsion demands by continuously monitoring battery SOC and processing the vehicle speed command to determine the appropriate operating mode. When SOC drops below a predefined threshold, the system activates the range extender unit, prompting the ICE to either shut down or operate steadily at 3000, its point of optimal efficiency.

The control architecture converts the target vehicle speed into a corresponding motor speed reference (rpm_ref), which is fed into a closed-loop torque-based speed control algorithm. This algorithm, using a PI controller, generates precise motor torque commands (T_ref) to ensure accurate speed tracking and compensate for dynamic load variations. During ICE activation, the generator requires an initial torque of 4 Nm to overcome static friction and rotational inertia before transitioning into power generation mode.

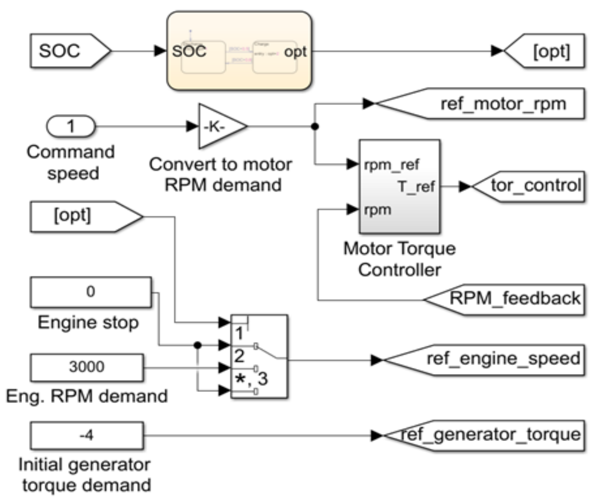

Figure 3. *The control strategy for the extended-range amphibious vehicle*

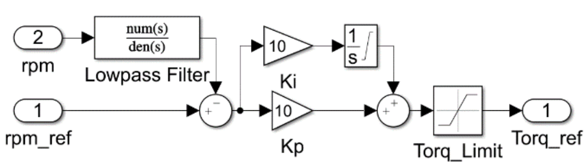

Figure 4. *The motor torque controller*

As shown in Figure 4, the motor torque controller compares the desired speed (rpm_ref) with the actual motor speed and uses a PI controller with predefined gains to compute the required torque output (Torq_ref). The system also incorporates signal filtering for stability and a torque limiter for protection, following a standard architecture widely adopted for motor speed regulation in automotive applications.

In this study, a permanent magnet synchronous motor (PMSM) was selected for the simulation model, as depicted in Figure 5. The torque signal is actively controlled to generate the necessary propulsion torque, enabling the vehicle to achieve the desired target speed.

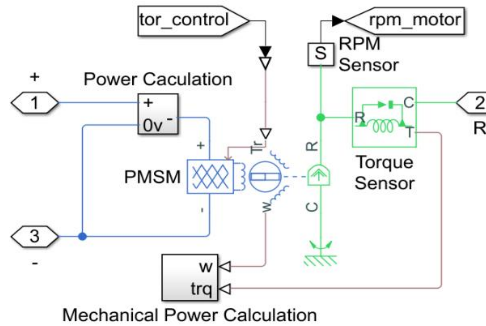

Figure 5. *Motor subsystem*

Figure 6 illustrates the vehicle body model developed in the Simulink environment. The model adopts a rear-wheel-drive configuration, in which a differential mechanism drives the two rear wheels, while the front wheels rotate freely. All four wheels are mechanically linked to the vehicle body, with key geometric parameters such as wheelbase, track width, and center of gravity position appropriately defined. To accurately capture nonlinear tire behavior, the Magic Formula tire model is employed. The vehicle speed is converted into the required electric motor speed (RPM) using drivetrain kinematic relationships, which serve as the primary input for the motor controller's speed regulation algorithm.

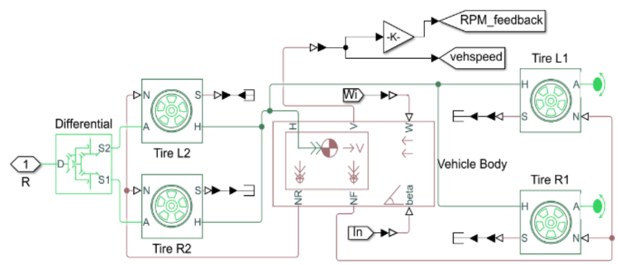

Figure 6. *The vehicle body subsystem*

3. Simulation results and discussion

The simulation utilizes a variable-step solver with automatic algorithm selection, configured with a sampling time of 0.1 seconds to ensure consistent data acquisition while maintaining numerical stability. Key solver settings include adaptive zero-crossing detection with a limit of 1000 events to handle discontinuities, and error control based on a relative tolerance of $1x10^{-6}$ combined with auto-scaled absolute tolerance. A step size of 0.1 seconds provides a balanced compromise between computational efficiency and dynamic resolution, making it suitable for real-time vehicle control simulations. This configuration is optimized for multi-domain systems, such as electromechanical powertrains, where accurate timing and transient response capture are critical. Additionally, the vehicle dynamics simulation assumes operation on dry asphalt with a rolling resistance coefficient of 0.013. The tire-road interaction is modeled using the Pacejka Magic Formula, with the following parameters: B = 10, C = 1.9, D = 1, and E = 0.97. The road surface is modeled as flat with zero gradient, and the effects of wind and other environmental factors are neglected. The simulation results presented in Figure 7 illustrate the vehicle's speed, distance traveled, and battery SOC. The findings indicate that the VCU effectively regulates the vehicle's speed, ensuring close adherence to the desired speed profile. The vehicle accelerates from 0 to 40 km/h in less than 16 seconds, achieving a maximum speed of 60 km/h, thereby meeting the design objectives. Assuming an initial battery SOC of 55%, after traveling approximately 18.6 km over a duration of 32 minutes (1939 seconds), the SOC drops below 50%. At this threshold, the ICE is activated to generate electrical power, both to recharge the battery and to sustain motor operation, enabling continuous vehicle movement. Under the specified speed conditions, the SOC reaches 52.6% after approximately 18 minutes of operation. The maximum charging rate is maintained at 0.2C, ensuring efficient battery recharging while preserving optimal system performance.

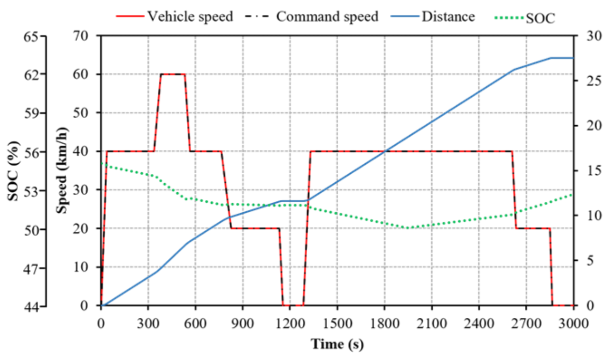

Figure 7. *Vehicle speed, travel distance, and battery state of charge*

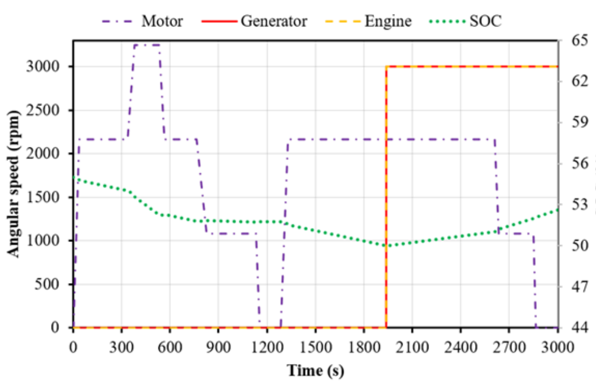

Figure 8. *Angular speed of devices*

Furthermore, the simulation results for the angular velocities of the electric motor, generator, and internal combustion engine demonstrated that the motor's rotational speed accurately follows the vehicle's speed profile, as shown in Figure 8. Due to the coupling between the motor and the wheel shaft, the motor speed is regulated to be higher than the wheel speed by a factor corresponding to the gear ratio of 6.12. The ICE and generator operate at synchronized speeds, initially remaining idle at 0 RPM and subsequently ramping up to 3000 RPM when the battery SOC drops below 50% (at approximately 1939 seconds). This coordinated operation facilitates efficient energy transfer, allowing the ICE and generator to work jointly in recharging the battery and supplying additional power to the electric motor as required. The implemented control strategy effectively regulates system performance, ensuring that energy management objectives are met while maintaining the desired dynamic behavior of the vehicle.

The simulation results for the power output of key components, including the electric motor, generator, internal combustion engine, and battery, are presented in Figure 9. The analysis demonstrates that motor power varies dynamically in response to changes in vehicle speed. During acceleration phases, the DC motor approaches its maximum power output, reaching approximately 3.8 kW when accelerating from 0 to 40 km/h and 4.4 kW when accelerating from 40 km/h to 60 km/h. At the maximum speed of 60 km/h, the motor power requirement stabilizes at approximately 2.5 kW. A notable observation is that during deceleration, the motor power transitions into the negative range, indicating that the motor is operating in generator mode. This regenerative braking mechanism converts kinetic energy into electrical energy, which is subsequently fed back into the battery, thereby improving overall energy efficiency. The battery power profile closely mirrors that of the motor, fluctuating in response to vehicle speed and motor power demands. During acceleration, the battery supplies substantial power to the motor, whereas during deceleration, it absorbs power from the regenerative braking process.

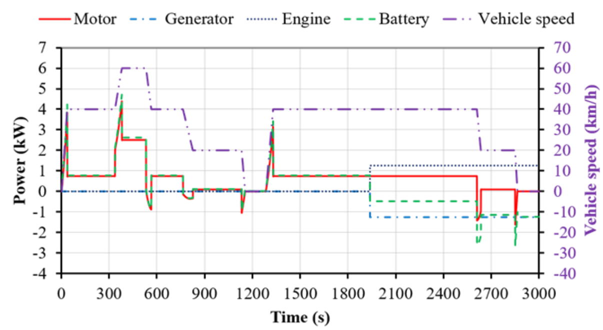

Figure 9. *Power generation and consumption of devices*

The power generation of the ICE is directly correlated with the generator's power output. The ICE is activated when the SOC falls below 50%, at which point it increases output to supply sufficient power to the generator. The generator subsequently converts this mechanical energy into electrical power, which is used to recharge the battery and, if necessary, support the electric motor's operation. This process ensures that the battery maintains an adequate charge level, enabling continuous and efficient vehicle operation. Overall, the results presented in Figure 5 illustrate the dynamic interaction between the motor, generator, ICE, and battery. By effectively managing power flow within the system, the vehicle meets its performance targets while optimizing energy efficiency and preserving battery health. This integrated approach is crucial for the successful operation of an extended-range electric vehicle, balancing speed, power demand, and energy management.

The charging and discharging voltage and current of the battery in relation to vehicle speed are illustrated in Figure 10. The simulation results of battery current and voltage during vehicle operation under the designed driving cycle indicate that battery voltage fluctuates in response to acceleration and deceleration. This behavior is attributed to variations in current demand as vehicle speed changes. In this simulation, the voltage drop was set at 0.01 V/A. A key observation is that during acceleration phases from 0 to 40 km/h and from 40 to 60 km/h, the maximum current supplied to the motor reached approximately 61 A and 69 A, respectively, both within the battery's maximum discharge current limit of 159 A. At constant speeds, the current required by the motor was approximately 10.8 A at 40 km/h and 37.4 A at 60 km/h. A negative current value indicates that energy is being recuperated and fed back into the battery through regenerative braking. Most of the charging current remained below the battery’s maximum allowable charging limit of 24 A (0.2C), ensuring safe and efficient recharging. When the vehicle was stationary, the maximum charging current reached approximately 17.2 A. This control strategy effectively regulates battery operation, preventing over-discharge and overcharging, thereby enhancing battery longevity and optimizing vehicle performance.

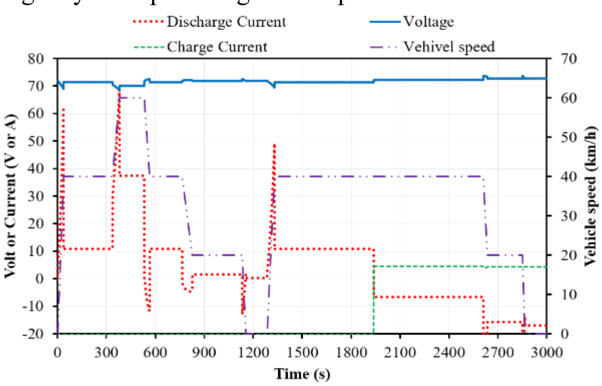

Figure 10. *Battery discharging voltage and current*

4. Conclusion

In this study, a novel design and modeling framework for an extended-range amphibious vehicle was developed using MATLAB/Simulink. The input parameters were systematically derived from both design requirements and specifications of commercially available components, ensuring practical feasibility. The proposed model enables comprehensive evaluation of the vehicle’s dynamic performance, with simulation results demonstrating that the system reliably achieves predefined speed profiles while maintaining effective power distribution. A key contribution of this work lies in the integration of energy management analysis under diverse driving conditions and battery charging strategies. The results highlight the vehicle's ability to operate within specified performance boundaries, optimize energy consumption, and preserve battery longevity through efficient charge-discharge control factors that are essential for extending driving range and reducing dependence on fossil fuels. The outcomes of this research establish a foundational framework for the advancement of energy-efficient electric mobility solutions capable of operating across diverse terrains, thereby contributing to the development of next-generation sustainable transportation systems.

Future work will focus on refining energy management strategies, enhancing control algorithms, and exploring advanced energy storage technologies to improve driving range and battery performance. Additionally, real-world testing and validation of the simulation results will be conducted, addressing energy losses, efficiency during power transitions, and performance under extreme conditions. The adaptability of the control strategy to various terrains and load conditions, as well as battery safety and lifespan, will also be further explored.

Acknowledgments: The authors gratefully acknowledge the support in terms of time and research facilities provided by Ho Chi Minh City University of Technology and Education (HCMUTE) and Nam Can Tho University (DNC) throughout this study. Additional support from Ho Chi Minh City University of Technology (HCMUT) and Vietnam National University Ho Chi Minh City (VNU-HCM) is also sincerely appreciated.

REFERENCES

[1] A. A. May, N. T. Nguyen, and A. A. Presto, “Gas-and particle-phase primary emissions from in use, on-road gasoline, and diesel vehicles”, *Atmospheric Environment*, vol. 88, no. 5, pp. 247-260, 2014. https://doi.org/10.1016/j.atmosenv.2014.01.046

[2] Q. Lin, X. Xu, T. Zou, and J. Yang, “Design and simulation of an extended-range dynamic system for an amphibious vehicle”, in *IOP Conference Series: Materials Science and Engineering*, St. Petersburg, Russian Federation, 2018, pp. 042153.

[3] M. Gawande and P. Mali, “Amphibious vehicle”, *International Research Journal of Engineering and Technology*, vol. 3, no. 10, pp. 137-138, 2016.

[4] D. Jiang, L. Huo, P. Zhang, and Z. Lv, “Energy-Efficient Heterogeneous Networking for Electric Vehicles Networks in Smart Future Cities”, *IEEE Trans. Intell. Transp. Syst., vol. 22, no. 3, pp.* 1868–1880. 2021. DOI: 10.1109/TITS.2020.3029015

[5] T. S. Castro, T. M. de Souza, and J. L. Silveira, “Feasibility of Electric Vehicle: Electricity by Grid × Photovoltaic Energy”, *Renewable and Sustainable Energy Reviews*, vol. 69, pp. 1077-1084, 2017. https://doi.org/10.1016/j.rser.2016.09.099

[6] O. Egbue and S. Long, “Barriers to widespread adoption of electric vehicles: An analysis of consumer attitudes and perceptions”, *Energy Policy*, vol. 48, pp. 717–729, 2012. https://doi.org/10.1016/j.enpol.2012.06.009

[7] M. Chen and J. J. Li, “Experimental study on heating performance of pure electric vehicle power battery under low-temperature environment”, *Int. J. Heat Mass Transfer,* vol. 172, pp. 121191, 2021. https://doi.org/10.1016/j.ijheatmasstransfer.2021.121191

[8] Y. Gao, X. Wang, G. Q. Shu, H. Tian, and X. L. Shi, “Applicability analysis of waste heat recovery technology and strategy exploration for hybrid electric vehicles under di-verse road conditions”, *Energy Conversion and Management,* vol. 230, pp. 113780, 2021. https://doi.org/10.1016/j.enconman.2020.113780

[9] Y. H. Xu *et al.*, “Experimental study on small power generation energy storage device based on pneumatic motor and compressed air”, *Energy Conversion and Management*, vol. 234, pp. 113949. 2021. https://doi.org/10.1016/j.enconman.2021.113949

[10] D. K. Shetty *et al.*, “Barriers to widespread adoption of plug-in electric vehicles in emerging Asian markets: An analysis of consumer behavioral attitudes and perceptions”, *Cogent Engineering*, vol. 7, no. 1, pp. 1796198, 2020. https://doi.org/10.1080/23311916.2020.1796198

[11] N. Powell *et al.*, “Auxiliary power units for range-extended electric vehicles”, in *proc. Sustainable Vehicle Technologies: Driving the green agenda*, Gaydon, Warwickshire, 2012, pp. 225-235.

[12] Y. Yang *et al.*, “Research on the energy management strategy of extended range electric vehicles based on a hybrid energy storage system”, *Energy Reports*, vol. 8, pp. 6602-6623, 2022. https://doi.org/10.1016/j.egyr.2022.05.013

[13] M. Ehsani, Y. Gao, S. Longo, and K. Ebrahimi, *Modern Electric, Hybrid Electric, and Fuel Cell Vehicles,* Third edition. Ohio: CRC Press, 2018.